A phosphorylation switch on RbBP5 regulates histone H3 Lys4 methylation

Pamela Zhang,[1] Chandra-Prakash Chaturvedi,[2,3] Veronique Tremblay,[1] Myriam Cramet,[1] Joseph S. Brunzelle,[4] Georgios Skiniotis,[5,6] Marjorie Brand,[2,3] Ali Shilatifard,[7] and Jean-François Couture[1]

[1]Department of Biochemistry, Microbiology, and Immunology, Ottawa Institute of Systems Biology, University of Ottawa, Ottawa, Ontario K1H 8M5, Canada; [2]The Sprott Center for Stem Cell Research, Regenerative Medicine Program, Ottawa Hospital Research Institute, Ottawa, Ontario K1H 8L6, Canada; [3]Department of Cellular and Molecular Medicine, University of Ottawa, Ontario K1H 8L6, Canada; [4]Department of Pharmacology, Feinberg School of Medicine, Northwestern University, Chicago, Illinois 60611, USA; [5]Life Sciences Institute, [6]Department of Biological Chemistry, University of Michigan, Ann Arbor, Michigan 48109, USA; [7]Department of Biochemistry and Molecular Genetics, Northwestern University, Chicago, Illinois 60611, USA

The methyltransferase activity of the trithorax group (TrxG) protein MLL1 found within its COMPASS (complex associated with SET1)-like complex is allosterically regulated by a four-subunit complex composed of WDR5, RbBP5, Ash2L, and DPY30 (also referred to as WRAD). We report structural evidence showing that in WRAD, a concave surface of the Ash2L SPIa and ryanodine receptor (SPRY) domain binds to a cluster of acidic residues, referred to as the D/E box, in RbBP5. Mutational analysis shows that residues forming the Ash2L/RbBP5 interface are important for heterodimer formation, stimulation of MLL1 catalytic activity, and erythroid cell terminal differentiation. We also demonstrate that a phosphorylation switch on RbBP5 stimulates WRAD complex formation and significantly increases KMT2 (lysine [K] methyltransferase 2) enzyme methylation rates. Overall, our findings provide structural insights into the assembly of the WRAD complex and point to a novel regulatory mechanism controlling the activity of the KMT2/COMPASS family of lysine methyltransferases.

Supplemental material is available for this article.

Received October 27, 2014; revised version accepted December 15, 2014.

The methyltransferase activity of the trithorax group (TrxG) protein MLL1 as well as the other members of the KMT2 (lysine [K] methyltransferase 2) family found within COMPASS (complex associated with SET1) catalyzes the site-specific methylation of the ε-amine of Lys4 (K4) of histone H3 (Shilatifard 2012). While these enzymes share the ability to methylate the same residue on histone H3, the catalytic activity of these enzymes is linked to different biological processes. MLL1/MLL2 di/trimethylate H3K4 (H3K4me2/3) and regulate *Hox* gene expression during embryonic development (Yu et al. 1995; Dou et al. 2006). MLL3/MLL4 regulate adipogenesis (Lee et al. 2008) and primarily monomethylate H3K4 (H3K4me1) at both enhancer (Herz et al. 2012; Hu et al. 2013) and promoter (Cheng et al. 2014) regions, while SET1A/B are the primary H3K4 trimethyltransferases (Wu et al. 2008). However, despite divergence in catalytic activity and functional roles, enzymes of the KMT2/COMPASS family must assemble into multisubunit complexes to carry out their biological functions.

Our molecular understanding of the protein complexes involved in H3K4 methylation stems from the isolation of COMPASS from *Saccharomyces cerevisiae* (Miller et al. 2001; Roguev et al. 2001; Krogan et al. 2002; Dehe et al. 2006). These studies demonstrated that regulatory subunits found within COMPASS and mammalian COMPASS-like complexes play key roles in stabilizing the enzyme and stimulating its methyltransferase activity as well as targeting the protein complex to specific genomic loci (Couture and Skiniotis 2013). While each of these multisubunit protein complexes contains unique subunits, each member of the KMT2 family associates with a common set of four evolutionarily conserved regulatory proteins; namely, WDR5, RbBP5, Ash2L, and DPY30 (WRAD) (Couture and Skiniotis 2013). The four-subunit complex directly binds the SET domain of KMT2 enzymes and serves as an essential modulatory platform stimulating the enzymatic activity of each member within this family (Dou et al. 2006; Steward et al. 2006; Patel et al. 2009; Avdic et al. 2011; Zhang et al. 2012).

In an attempt to understand the structural mechanisms underlying the assembly of the WRAD complex and stimulation of MLL1 methyltransferase activity, several studies have dissected the structure and function of each WRAD subunit (Couture and Skiniotis 2013). WDR5 is crucial for the structural integrity of the complex and acts as a bridge linking each member of the KMT2 family (Dharmarajan et al. 2012; Zhang et al. 2012) to the regulatory subunits RbBP5, Ash2L, and DPY-30 (Odho et al. 2010; Avdic et al. 2011). In RbBP5, a predicted unstructured region binds to Ash2L and WDR5 and is important for the stimulation of MLL1 methyltransferase activity (Cao et al. 2010; Avdic et al. 2011). Furthermore, mapping analysis has identified that this region of RbBP5 binds to the SPIa and ryanodine receptor (SPRY) domain of Ash2L (Chen et al. 2012); however, the structural basis underlying the interaction of RbBP5 with Ash2L is unknown.

Here, we report the crystal structure of the Ash2L SPRY domain in complex with RbBP5. We show that Ash2L–RbBP5-binding specificity is conferred by several conserved residues on both Ash2L and RbBP5. Structure-

[*Keywords*: COMPASS; chromatin; epigenetics; histone H3 Lys4; methylation]
Corresponding author: jean-francois.couture@uottawa.ca
Article is online at http://www.genesdev.org/cgi/doi/10.1101/gad.254870.114.

guided mutational analysis reveals that disruption of this binding interface impairs formation of the WRAD complex, stimulation of MLL1 methyltransferase activity, and terminal differentiation of erythroid cells. Interestingly, the structure reveals that a phosphorylation switch on RbBP5 stimulates WRAD complex formation and increases methylation of H3K4 by KMT2 enzymes.

Results and Discussion

Crystal structure of Ash2L in complex with RbBP5

After determining that the Ash2L SPRY domain binds residues 344–364 of RbBP5 (Supplemental Fig. S1), we sought to gain structural insights into the interaction between Ash2L and RbBP5 and solved the crystal structure of Ash2L^{SPRYdel} in complex with a peptide corresponding to residues 344–357 of RbBP5 at a resolution of 2.20 Å (Supplemental Table S1). The Ash2L^{SPRYdel} domain adopts a twisted β sandwich composed of two antiparallel β sheets (referred to as A and B). Sheet A is composed of β2, β4, β5, β6, β7, and β11, while sheet B is composed of β1, β3, β8, β9, β10, and β12. The two sheets are linked by several interconnecting loops of varying length that extend out of the β-sandwich fold, and the Ash2L^{SPRYdel} domain ends with a short α helix (α1) (Fig. 1A).

Simulated annealing omit maps reveal clear electron density for the RbBP5 peptide, including residues 345–354 (Supplemental Fig. S2A). No electron density is observed for the RbBP5 E344 side chain (single letter denotes RbBP5 residues) and residues 355–357, and therefore they are not modeled in the structure. The RbBP5 peptide adopts a chair-like conformation and sits on a shallow surface formed by β4–β5–β6–β7 of sheet A. The N-terminal half of the peptide (residues 344–348) adopts an elongated conformation and protrudes perpendicularly down toward the basic surface of the Ash2L SPRY domain (Fig. 1A,B). In this region of the peptide, the RbBP5 E347 side chain makes van der Waals contacts with the backbone of Ash2L residues forming the β1–β2 loop, while the R348 side chain is solvent-exposed. In stark contrast, the E349 side chain binds in a deep pocket formed by the side chains of Tyr313 and Arg367 (Fig. 1A, C). The main chain carbonyl of E349 makes a hydrogen bond with the Ash2L Tyr313 hydroxyl group, while its carboxylate group engages in several hydrogen bonds with the guanidium group of Arg367. Located in the bulge of the S-shaped conformation, the F352 phenyl side chain makes hydrophobic contacts with Tyr313, Pro356, and Tyr359 side chains. Similar to E349, the D353 carboxylate group makes two hydrogen bonds with the Arg343 guanidium group, suggesting that the Ash2L^{SPRY} positively charged cleft is important for binding this region predominantly occupied by glutamic acid and aspartic acid residues (subsequently referred to as the D/E box) of RbBP5 (Fig. 1B,C).

Disruption of Ash2L/RbBP5 interaction impairs MLL1 enzymatic stimulation and delays erythroid cell terminal differentiation

Following structural analysis of the Ash2L/RbBP5 complex, we first sought to identify Ash2L residues that are key for binding to RbBP5. Using isothermal titration calorimetry (ITC) (Fig. 2A; Supplemental Fig. S3A), we found that replacement of Tyr313 and Arg343—two

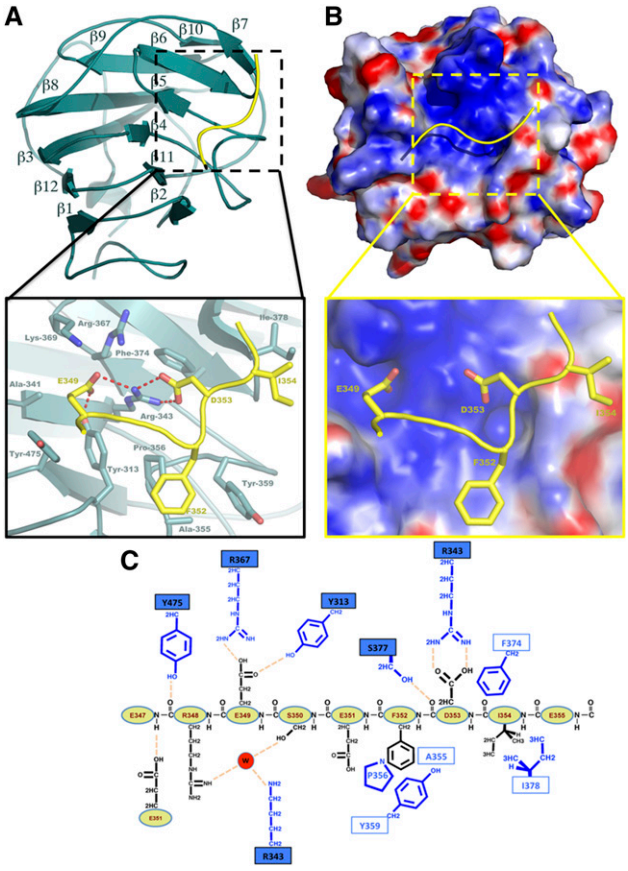

Figure 1. The ASH2L SPRY domain binds a D/E box on RbBP5. (*A*) Cartoon representation of the Ash2L SPRY domain (green) in complex with RbBP5 (yellow) and a zoomed view on the interactions between the ASH2L SPRY domain and RbBP5. Ash2L and RbBP5 carbon atoms are highlighted in light green and yellow, respectively. Key hydrogen bonds are rendered as red dashed lines. For clarity, only a subset of interactions is shown. (*B*) Electrostatic potentials are contoured from -10 kbTe^{-1} (red) to +10 kbTe^{-1} (blue). (e) Charge of an electron; (kb) Bolzmann's constant; (T) temperature in Kelvin. Zoomed view is on the positively charged cleft of Ash2L. (*C*) Schematic representation of the interactions stabilizing RbBP5 into the Ash2L SPRY peptide-binding pocket. Yellow spheres represent RbBP5 residues. Ash2L residues making hydrogen bonds (filled boxes), hydrophobic contacts, or van der Waals contacts (empty boxes) with RbBP5 are rendered in blue. Hydrogen bonds are highlighted as orange dashed lines. For clarity, some interactions were omitted from the figure.

residues lining the base of the Ash2L^{SPRY} D/E-binding pocket and interacting with RbBP5 E347 and D353, respectively—with alanine severely impaired binding of RbBP5. Accordingly, enzymatic assays performed with the same mutants resulted in an approximately fivefold reduction of MLL1 methyltransferase activity compared with wild-type Ash2L (Fig. 2B; Supplemental Fig. S3B). Mutation of Pro356 and Arg367, residues interacting with the hydrophobic bulge and E349 of the RbBP5 D/E box, resulted in sixfold and 13-fold reduction in binding, respectively. Accordingly, reconstitution of the complex with the Ash2L Pro356Ala and Arg367Ala mutants failed to stimulate MLL1 methyltransferase activity to the same extent as wild-type Ash2L, demonstrating that an Ash2L positively charged pocket lined by hydrophobic residues is important for WRAD assembly and MLL1 methyltransferase activity (Fig. 2A,B).

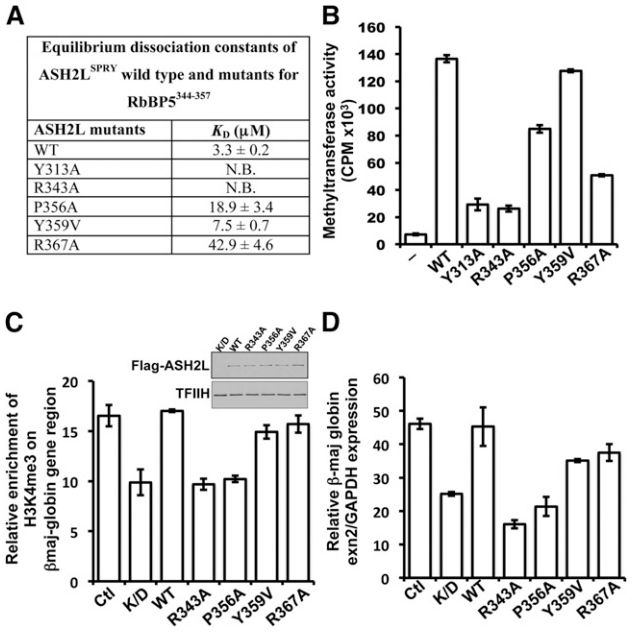

Figure 2. Interaction between Ash2L and RbBP5 is essential for terminal differentiation of erythroid cells. (*A*) Dissociation constants determined using ITC as performed in Supplemental Figure S1C. (*B*) Methyltransferase assays performed with MLL1 3762–3969 alone (−) or in the presence of wild-type Ash2L (+) (WT) or the indicated mutants. (*C*) Mutation of Ash2L SPRY surface residues prevents maximal H3K4me3 at the *β-globin* LCR. Enrichment of H3K4me3 was measured by chromatin immunoprecipitation (ChIP) as previously described (Sarvan et al. 2011) with either the empty vector (K/D) or constructs corresponding to Ash2L wild type or Ash2L R343A, P356A, Y359V, or R367A mutants. The *inset* illustrates a Western blot of endogenous Ash2L knockdown and rescue with shRNA-resistant Flag-tagged Ash2L wild type or mutants in differentiated MEL cells in which TFIIH p89 was used as a loading control. (*D*) Interactions between Ash2L and RbBP5 are important for *β-globin* gene expression. Transcription of the *β-major globin* gene (*βmaj-globin*) versus glyceraldehyde-3-phosphate dehydrogenase (GAPDH) was assessed using quantitative RT–PCR as previously described (Demers et al. 2007).

Ash2L is essential for maintaining high levels of histone H3K4 trimethylation (Steward et al. 2006; Demers et al. 2007), and knockdown of Ash2L in murine erythroid leukemia (MEL) cells results in a decrease of the H3K4me3 mark at the hypersensitive site 2 (HS2) of the *β-globin* locus control region (LCR) and a concomitant loss of *β-globin* gene transcription, a marker of erythroid cell terminal differentiation (Demers et al. 2007). To test the impact of mutations impairing Ash2L/RbBP5 complex formation, we transfected Flag-tagged constructs corresponding to the Ash2L wild type and single-point mutant of residues forming the base of the RbBP5-binding pocket in MEL cells stably expressing a doxycycline (Dox)-inducible shRNA directed against Ash2L (Demers et al. 2007). Treatment of cells with Dox resulted in a 40% decrease of H3K4me3 at the HS2 locus and a corresponding loss of 50% in *β-globin* gene expression (Fig. 2C,D). Transfection of MEL cells with small hairpin-resistant Flag-Ash2L^{WT} restored H3K4me3 and transcription of the *β-globin* gene to wild-type levels. Consistent with our binding and methyltransferase assays, Flag-Ash2L^{Arg343ALa} and Flag-Ash2L^{Pro356Ala} mutants failed to maintain maximal expression of the *β-globin* gene (Fig. 2C,D) and rescue the loss of H3K4me3. Correlatively, transfection of Flag-ASH2L^{Tyr359Val}, a mutant that exhibited activity similar to Ash2L^{WT}, restored H3K4me3 and *β-globin* gene expression levels similar to Ash2L^{WT}. Together, our findings strongly suggest that a functional Ash2L/RbBP5 heterodimer is pivotal for maintaining the differentiation potential of MEL cells.

Phosphorylation of RbBP5 on S350 potentiates WRAD assembly

MLL1 is tightly regulated by various mechanisms, including allosteric regulation by the WRAD complex (Dou et al. 2006), deposition of other post-translational modifications on histone proteins (Southall et al. 2009), and phosphorylation of MLL1 by ATR (Liu et al. 2010). In the RbBP5 D/E box (Supplemental Fig. S4), an evolutionarily conserved serine residue (S350) is found in the center of the Ash2L SPRY concave surface (Fig. 3A). Interestingly, three independent studies revealed that RbBP5 S350 is phosphorylated in vivo (Christensen et al. 2010; Phanstiel et al. 2011; Shiromizu et al. 2013). To determine the impact of RbBP5 phosphorylation on WRAD formation, we ectopically expressed constructs corresponding to either wild-type RbBP5 or an RbBP5 S350A mutant in fusion with a Flag tag in HEK293 cells. While we observed enrichment of Ash2L following immunoprecipitation of wild-type Flag-RbBP5, incubation of Flag-RbBP5 S350A with M2 agarose beads failed to coimmunoprecipitate Ash2L (Fig. 3B). Our findings that S350 does not make significant interactions with Ash2L (Fig. 3C) and that its substitution to alanine impairs WRAD assembly suggest that keeping the hydroxyl group on S350 is essential for high-affinity interaction between Ash2L and RbBP5. We next used ITC to determine the impact of S350 phosphorylation on the binding of RbBP5 to Ash2L and found that the phosphorylated peptide RbBP5$^{344-357}$ bound to Ash2L^{SPRY} with 15-fold higher affinity (Fig. 3D), strongly suggesting that the Ash2L SPRY domain is a novel phospho-reader domain.

To understand the structural basis underlying the binding preference of Ash2L to RbBP5^{phos}, we solved the crystal structure of the Ash2L/RbBP5^{phos} complex. The Ash2L/RbBP5^{phos} complex aligns with the Ash2L/RbBP5 with a root mean square deviation of 0.192 Å, suggesting that binding of RbBP5^{phos} does not induce large structural reorganization of the Ash2L SPRY domain compared with the unmodified complex. However, the phosphate moiety displaces the Lys369 side chain of Ash2L to accommodate short water-mediated hydrogen bonds with the phosphate group (Fig. 3E), demonstrating the ability of the Ash2L SPRY domain to read the phosphorylated form of RbBP5.

RbBP5 phosphorylation: a novel regulatory switch controlling WRAD assembly

With prior studies showing that the Ash2L C4-Winged-Helix (C4-WH) domain is important for binding to DNA (Chen et al. 2011; Sarvan et al. 2011) and ubiquitin (Wu et al. 2013) and that its SDI motif is important for binding to DPY-30 (South et al. 2010; Chen et al. 2012), our results point to a model in which Ash2L acts as a modulatory platform enabling the integration of a cascade of binding events that ultimately lead to the precise regulation of KMT2 methyltransferase activity. Here we report that Ash2L also recognizes the phosphorylated form of RbBP5. Binding and structural studies show that the Ash2L SPRY

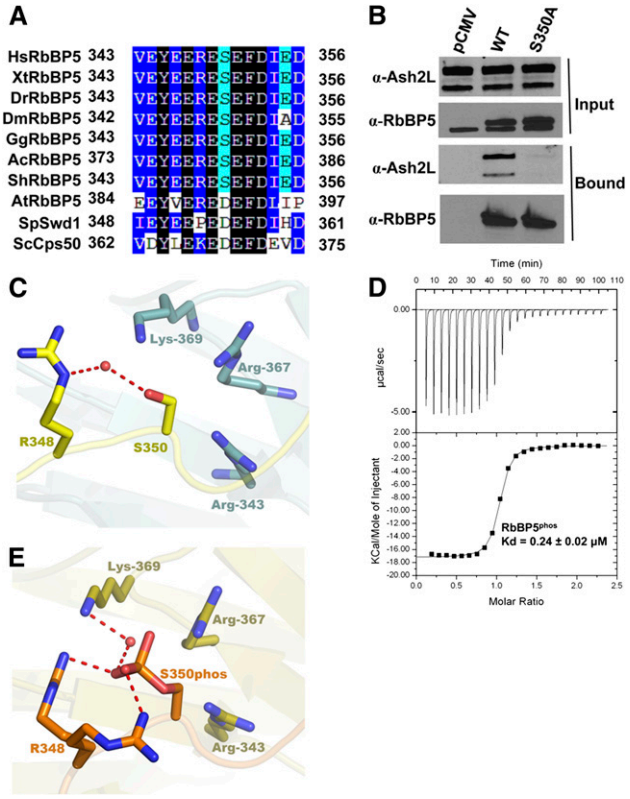

Figure 3. Phosphorylation of RbBP5 stimulates WRAD complex formation. (*A*) The RbBP5 D/E box is evolutionarily conserved. Sequence alignment of the RbBP5 D/E box from *Homo sapiens* (Hs), *Xenopus tropicalis* (Xt), *Dario rerio* (Dr), *Drosophila melanogaster* (Dm), *Gallus gallus* (Gg), *Anolis carolinensis* (Ac), *Sarcophilus harrisii* (Sh), *Arabidopsis thaliana* (At), *Schizosaccharomyces pombe* (Sp), and *Saccharomyces cerevisae* (Sc). Positions with 100%, 99%–75%, and <75% of amino acid conservation are represented in black, blue, and cyan, respectively. (*B*) Replacement of S350 to alanine decreases the interaction between RbBP5 and Ash2L. Immunoprecipitation of ectopically expressed Flag-tagged constructs of RbBP5 wild type and S350A with M2 agarose beads. RbBP5 and Ash2L were detected with the indicated antibodies. (*C*) Zoomed view of RbBP5 S350. Residues are colored as in Figure 1. (*D*) Phosphorylated RbBP5 binds Ash2L with higher affinity. Representative ITC experiment of RbBP5^{phos} binding to Ash2L. Data are shown as in Supplemental Figure S1C. (*E*) Crystal structure of Ash2L in complex with RbBP5^{phos}. Zoomed view of phosphorylated S350 in which RbBP5^{phos} and Ash2L carbon atoms are rendered in orange and dark yellow, respectively. Hydrogen bonds are illustrated as in Figure 1A.

domain binds RbBP5^{phos} with 15-fold more affinity and that the phosphate moiety induces local structural reorganization within Ash2L, suggesting that the Ash2L SPRY domain is a novel phospho-binding domain. However, the recognition of the phosphate moiety by Ash2L differs from other known phospho-readers. This is particularly apparent for 14-3-3 proteins, which engage in several electrostatic interactions with the phosphate moiety within a well-defined basic pocket (Rittinger et al. 1999). Consistently, Muslin et al. (1996) showed that 14-3-3 can only bind to a Ser259-phosphorylated form of a Raf-1 peptide. Our observations that Ash2L engages in a relatively small number of contacts with the phosphate moiety of S350 and binds to both the unmodified and phosphorylated forms of RbBP5 suggest that this mode of phosphopeptide recognition serves as a rheostat modulating WRAD complex formation rather than an on/off switch assigned to other canonical phospho-readers.

RbBP5 phosphorylation controls histone H3K4 methylation by KMT2 enzymes

Our studies revealed that RbBP5 phosphorylation creates a better epitope for the binding of the Ash2L SPRY domain. However, close inspection of the structure revealed that the RbBP5 phosphate moiety is not entirely buried within the SPRY concave surface (Fig. 4A), suggesting that it may potentially play a direct role in regulating the methyltransferase activity of the KMT2 enzymes. To address this question, we performed pull-down experiments with His-SUMO-tagged MLL3 bound to TALON beads and Ash2L/RbBP5 or Ash2L/RbBP5^{phos}. Following several washes, TALON-bound protein complexes were eluted with sample loading buffer, resolved on SDS-PAGE, and stained with Coomassie. Consistent with recent binding studies (Cao et al. 2010), we observed binding of the Ash2L/RbBP5 heterodimer to the MLL3 SET domain. Interestingly, a fivefold increase in binding was observed when the Ash2L/RbBP5^{phos} complex was incubated with His-SUMO-MLL3 (Fig. 4B), suggesting that the Ash2L/RbBP5^{phos} dimer serves as a better interacting platform for the binding of the MLL3 SET domain.

Based on these observations, we surmised that Ash2L/RbBP5^{phos} might modulate the methyltransferase activity of KMT2 enzymes. To confirm this hypothesis, enzymatic assays were performed with different concentrations of the MLL3 SET domain incubated with stoichiometric amounts of Ash2L/RbBP5 or Ash2L/RbBP5^{phos}. As shown in Figure 4C and consistent with previous studies (Zhang et al. 2012), both complexes stimulated MLL3 methyltransferase activity at 1 µM. However, upon dilution of the complex, Ash2L/RbBP5 failed to stimulate the activity of MLL3, while Ash2L/RbBP5^{phos} retained full activity of MLL3, demonstrating that RbBP5 phosphorylation serves as a rheostat increasing MLL3 kinetics.

After determining the impact of RbBP5 phosphorylation on MLL3 kinetics, we sought to determine the degree of K4 methylation catalyzed by MLL1 and MLL3 in the presence of the Ash2L/RbBP5 heterodimer reconstituted with RbBP5 or RbBP5^{phos}. We conducted enzymatic assays and subjected aliquots of the reactions to electrospray ionization mass spectrometry (ESI-MS). In comparison with the control reactions (Fig. 4D; Supplemental Fig. S5), a shift in the mass from 2346 to 2360 was measured for MLL1 and MLL3 in the presence of the Ash2L/RbBP5 heterodimer, corresponding to the transfer of a single methyl group to the ε-amine of K4. However, in contrast to the assays performed with unmodified RbBP5, we observed a sharp increase in H3K4me1 when the assays were performed with the Ash2L/RbBP5 heterodimer reconstituted with RbBP5^{phos} (Fig. 4D). The time course of the methylation reactions followed by ESI-MS further showed that the MLL3/Ash2L/RbBP5^{phos} robustly methylates a histone H3 peptide when compared with MLL3 incubated with the unphosphorylated Ash2L/RbBP5 heterodimer (Fig. 4D). Interestingly, we also observed detectable levels of H3K4me2 for both MLL1 and MLL3 (Fig. 4D; Supplemental Fig. S4), suggesting that the enhancement of MLL3 catalytic activity, a predominant histone H3K4 monomethyltransferase, by the Ash2L/RbBP5^{phos} complex pushes the reaction further to observe H3K4me2. Intriguingly, methyltransferase

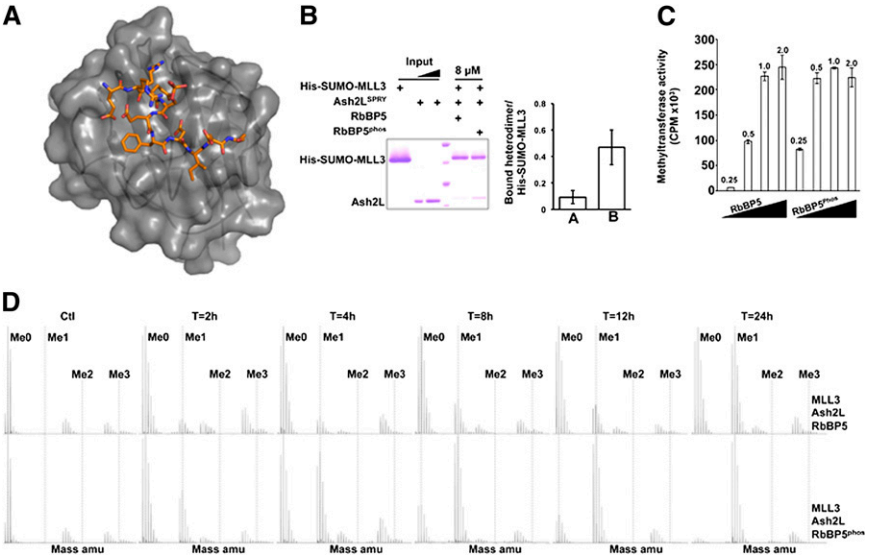

Figure 4. RbBP5 S350 phosphorylation increases the catalytic activity of MLL3. (*A*) Surface representation of the Ash2L SPRY domain in complex with RbBP5^{phos}. The Ash2L surface is highlighted in gray, and RbBP5 is colored as in Figure 3E. (*B*) Pull-down assays of the Ash2L/RbBP5 or Ash2L/RbBP5^{phos} complexes by the MLL3 SET domain. Bound proteins were separated on SDS-PAGE and detected by Coomassie staining. A representative Coomassie-stained SDS-PAGE gel is shown at the *left*, and the quantified mean of bound Ash2L/RbBP5 (*A*) or Ash2L/RbBP5^{phos} (*B*) complexes normalized to MLL3 is shown at the *right* ($n = 3$ experiments; $P < 0.05$). (*C*) Methyltransferase assays were performed with increasing amounts (indicated at the *top* of each graph bar [in micromolar]) of MLL3 and Ash2L/RbBP5 or Ash2L/RbBP5^{phos}. Assays were performed as in Supplemental Figure S1B. (*D*) Representative spectra of ESI-MS experiments performed with MLL3 incubated with Ash2L/RbBP5 (*top*) or Ash2L/RbBP5^{phos} (*bottom*) complexes. The duration of the experiments is indicated at the *top* of each panel.

assays performed with a higher concentration of MLL3 reconstituted with the Ash2L/RbBP5 or Ash2L/RbBP5^{phos} showed that both complexes efficiently trimethylate H3K4 but failed to show increased rates of di- and trimethylation of histone H3K4 by the MLL3/Ash2L/RbBP5^{phos} complex (Supplemental Fig. S5). Overall, our observations strongly suggest that RbBP5 phosphorylation couples the assembly of the WRAD complex to the allosteric regulation of KMT2 enzymes.

Enzymatic assays revealed that MLL3 monomethylates H3K4 in the presence of Ash2L/RbBP5 reconstituted with unmodified RbBP5. These observations are consistent with recent studies showing that COMPASS-like MLL3/MLL4 complexes predominantly monomethylate H3K4 at enhancer regions and specific promoter regions (Herz et al. 2012; Hu et al. 2013; Morgan and Shilatifard 2013; Cheng et al. 2014). Interestingly, upon incubation of the MLL3 SET domain with the Ash2L/RbBP5 complex reconstituted with RbBP5^{phos}, peaks corresponding to H3K4me1 and H3K4me2 were observed. In addition, a peak corresponding to H3K4me3 was also observed when experiments were performed with a higher concentration of MLL3 complexes. These observations are also consistent with recent studies showing that deletion of MLL3 in NIH3T3-L1 cells results in a significant loss of H3K4me3 at the promoter region of the adipogenic marker gene *aP2* (Lee et al. 2008). Moreover, B-cell-specific knockout of PTIP, a subunit associating with MLL3/MLL4 complexes (Cho et al. 2007; Issaeva et al. 2007), results in a loss of H3K4me3 at specific Igh switch regions upon LPS stimulation (Daniel et al. 2010). These seemingly contrasting results potentially point to a model in which RbBP5 phosphorylation can act as a switch increasing MLL3 kinetics, facilitating the formation of H3K4me1 that can potentially be further methylated to ultimately form H3K4me2/3. Analogous to the differences in activity between members of the KMT2 family of enzyme, our observations suggest that at least two populations of the WRAD complex exist in cells tailored to performed distinct functions.

Materials and methods

Protein crystallization and structure determination

Recombinantly purified Ash2L^{SPRYdel} (5–10 mg/mL) (see the Supplemental Material) was incubated with equimolar amounts of RbBP5 344–357 for 1 h on ice and crystallized using the sitting drop vapor diffusion method at 18°C. Diffraction-quality crystals were obtained in 0.2 M magnesium chloride hexahydrate, 0.1 M Bis-Tris (pH 5.5), and 25% (w/v) polyethylene glycol. The crystals were sequentially soaked in the mother liquor supplemented with an increasing amount (5%–20%) of glycerol, harvested, and flash-frozen in liquid nitrogen. The structure was solved by molecular replacement, and model building was performed as detailed in the Supplemental Material.

ITC, in vitro methyltransferase assays, and ESI-MS

ITC experiments and enzymatic assays were performed as previously described (Zhang et al. 2012). ESI-MS analysis was performed at the SPARC BioCentre using a QSTAR Elite and is detailed in the Supplemental Material.

MEL cells

MEL cells were transfected with plasmids expressing Flag-only, Flag-Ash2L wild type, Flag-Ash2L Y313A, Flag-Ash2L R343A, Flag-Ash2L P356A, Flag-Ash2L Y359V, and Flag-Ash2L R367A by electroporation. Twelve hours after transfection, differentiation was induced with DMSO as previously described (Demers et al. 2007). After 2 d, cells were pelleted by centrifugation, resuspended, and cross-linked as previously described (Demers et al. 2007). Chromatin extraction and immunoprecipitation experiments were performed as previously described (Sarvan et al. 2011) and quantified as detailed in the Supplemental Material.

Acknowledgments

P.Z. is supported by a Canadian Institutes of Health Research (CIHR) Banting and Best scholarship. J.-F.C. is supported by a CIHR grant (MOP-136816). This study was also supported by grants from the CIHR to M.B. (MOP-89834), and the National Institutes of Health to A.S. (R01GM069905). G.S. acknowledges support from the Pew Scholars Program in Biomedical Sciences.

References

Allis CD, Berger SL, Cote J, Dent S, Jenuwien T, Kouzarides T, Pillus L, Reinberg D, Shi Y, Shiekhattar R, et al. 2007. New nomenclature for chromatin-modifying enzymes. *Cell* **131:** 633–636.

Avdic V, Zhang P, Lanouette S, Groulx A, Tremblay V, Brunzelle J, Couture JF. 2011. Structural and biochemical insights into MLL1 core complex assembly. *Structure* **19:** 101–108.

Cao F, Chen Y, Cierpicki T, Liu Y, Basrur V, Lei M, Dou Y. 2010. An Ash2L/RbBP5 heterodimer stimulates the MLL1 methyltransferase activity through coordinated substrate interactions with the MLL1 SET domain. *PLoS ONE* **5:** e14102.

Chen Y, Wan B, Wang KC, Cao F, Yang Y, Protacio A, Dou Y, Chang HY, Lei M. 2011. Crystal structure of the N-terminal region of human Ash2L shows a winged-helix motif involved in DNA binding. *EMBO Rep* **12:** 797–803.

Chen Y, Cao F, Wan B, Dou Y, Lei M. 2012. Structure of the SPRY domain of human Ash2L and its interactions with RbBP5 and DPY30. *Cell Res* **22:** 598–602.

Cheng J, Blum R, Bowman C, Hu D, Shilatifard A, Shen S, Dynlacht BD. 2014. A role for H3K4 monomethylation in gene repression and partitioning of chromatin readers. *Mol Cell* **53:** 979–992.

Cho YW, Hong T, Hong S, Guo H, Yu H, Kim D, Guszczynski T, Dressler GR, Copeland TD, Kalkum M, et al. 2007. PTIP associates with MLL3- and MLL4-containing histone H3 lysine 4 methyltransferase complex. *J Biol Chem* **282:** 20395–20406.

Christensen GL, Kelstrup CD, Lyngso C, Sarwar U, Bogebo R, Sheikh SP, Gammeltoft S, Olsen JV, Hansen JL. 2010. Quantitative phosphoproteomics dissection of seven-transmembrane receptor signaling using full and biased agonists. *Mol Cell Proteomics* **9:** 1540–1553.

Couture JF, Skiniotis G. 2013. Assembling a COMPASS. *Epigenetics* **8:** 349–354.

Daniel JA, Santos MA, Wang Z, Zang C, Schwab KR, Jankovic M, Filsuf D, Chen HT, Gazumyan A, Yamane A, et al. 2010. PTIP promotes chromatin changes critical for immunoglobulin class switch recombination. *Science* **329:** 917–923.

Dehe PM, Dichtl B, Schaft D, Roguev A, Pamblanco M, Lebrun R, Rodríguez-Gil A, Mkandawire M, Landsberg K, Shevchenko A, et al. 2006. Protein interactions within the Set1 complex and their roles in the regulation of histone 3 lysine 4 methylation. *J Biol Chem* **281:** 35404–35412.

Demers C, Chaturvedi CP, Ranish JA, Juban G, Lai P, Morle F, Aebersold R, Dilworth FJ, Groudine M, Brand M. 2007. Activator-mediated recruitment of the MLL2 methyltransferase complex to the β-globin locus. *Mol Cell* **27:** 573–584.

Dharmarajan V, Lee JH, Patel A, Skalnik DG, Cosgrove MS. 2012. Structural basis for WDR5 interaction (Win) motif recognition in human SET1 family histone methyltransferases. *J Biol Chem* **287:** 27275–27289.

Dou Y, Milne TA, Ruthenburg AJ, Lee S, Lee JW, Verdine GL, Allis CD, Roeder RG. 2006. Regulation of MLL1 H3K4 methyltransferase activity by its core components. *Nat Struct Mol Biol* **13:** 713–719.

Herz HM, Mohan M, Garruss AS, Liang K, Takahashi YH, Mickey K, Voets O, Verrijzer CP, Shilatifard A. 2012. Enhancer-associated H3K4 monomethylation by Trithorax-related, the *Drosophila* homolog of mammalian Mll3/Mll4. *Genes Dev* **26:** 2604–2620.

Hu D, Gao X, Morgan MA, Herz HM, Smith ER, Shilatifard A. 2013. The MLL3/MLL4 branches of the COMPASS family function as major histone H3K4 monomethylases at enhancers. *Mol Cell Biol* **33:** 4745–4754.

Issaeva I, Zonis Y, Rozovskaia T, Orlovsky K, Croce CM, Nakamura T, Mazo A, Eisenbach L, Canaani E. 2007. Knockdown of ALR (MLL2) reveals ALR target genes and leads to alterations in cell adhesion and growth. *Mol Cell Biol* **27:** 1889–1903.

Krogan NJ, Dover J, Khorrami S, Greenblatt JF, Schneider J, Johnston M, Shilatifard A. 2002. COMPASS, a histone H3 (lysine 4) methyltransferase required for telomeric silencing of gene expression. *J Biol Chem* **277:** 10753–10755.

Lee J, Saha PK, Yang QH, Lee S, Park JY, Suh Y, Lee SK, Chan L, Roeder RG, Lee JW. 2008. Targeted inactivation of MLL3 histone H3-Lys-4 methyltransferase activity in the mouse reveals vital roles for MLL3 in adipogenesis. *Proc Natl Acad Sci* **105:** 19229–19234.

Liu H, Takeda S, Kumar R, Westergard TD, Brown EJ, Pandita TK, Cheng EHY, Hsieh JJD. 2010. Phosphorylation of MLL by ATR is required for execution of mammalian S-phase checkpoint. *Nature* **467:** 343–346.

Miller T, Krogan NJ, Dover J, Erdjument-Bromage H, Tempst P, Johnston M, Greenblatt JF, Shilatifard A. 2001. COMPASS: a complex of proteins associated with a trithorax-related SET domain protein. *Proc Natl Acad Sci* **98:** 12902–12907.

Morgan MA, Shilatifard A. 2013. Drosophila SETs its sights on cancer: Trr/MLL3/4 COMPASS-like complexes in development and disease. *Mol Cell Biol* **33:** 1698–1701.

Muslin AJ, Tanner JW, Allen PM, Shaw AS. 1996. Interaction of 14-3-3 with signaling proteins is mediated by the recognition of phosphoserine. *Cell* **84:** 889–897.

Odho Z, Southall SM, Wilson JR. 2010. Characterization of a novel WDR5-binding site that recruits RbBP5 through a conserved motif to enhance methylation of histone H3 lysine 4 by mixed lineage leukemia protein-1. *J Biol Chem* **285:** 32967–32976.

Patel A, Dharmarajan V, Vought VE, Cosgrove MS. 2009. On the mechanism of multiple lysine methylation by the human mixed lineage leukemia protein-1 (MLL1) core complex. *J Biol Chem* **284:** 24242–24256.

Phanstiel DH, Brumbaugh J, Wenger CD, Tian S, Probasco MD, Bailey DJ, Swaney DL, Tervo MA, Bolin JM, Ruotti V, et al. 2011. Proteomic and phosphoproteomic comparison of human ES and iPS cells. *Nat Methods* **8:** 821–827.

Rittinger K, Budman J, Xu J, Volinia S, Cantley LC, Smerdon SJ, Gamblin SJ, Yaffe MB. 1999. Structural analysis of 14-3-3 phosphopeptide complexes identifies a dual role for the nuclear export signal of 14-3-3 in ligand binding. *Mol Cell* **4:** 153–166.

Roguev A, Schaft D, Shevchenko A, Pijnappel WW, Wilm M, Aasland R, Stewart AF. 2001. The *Saccharomyces cerevisiae* Set1 complex includes an Ash2 homologue and methylates histone 3 lysine 4. *EMBO J* **20:** 7137–7148.

Sarvan S, Avdic V, Tremblay V, Chaturvedi CP, Zhang P, Lanouette S, Blais A, Brunzelle JS, Brand M, Couture JF. 2011. Crystal structure of the trithorax group protein ASH2L reveals a forkhead-like DNA binding domain. *Nat Struct Mol Biol* **18:** 857–859.

Shilatifard A. 2012. The COMPASS family of histone H3K4 methylases: mechanisms of regulation in development and disease pathogenesis. *Annu Rev Biochem* **81:** 65–95.

Shiromizu T, Adachi J, Watanabe S, Murakami T, Kuga T, Muraoka S, Tomonaga T. 2013. Identification of missing proteins in the neXtProt database and unregistered phosphopeptides in the PhosphoSitePlus database as part of the Chromosome-centric Human Proteome Project. *J Proteome Res* **12:** 2414–2421.

South PF, Fingerman IM, Mersman DP, Du HN, Briggs SD. 2010. A conserved interaction between the SDI domain of Bre2 and the Dpy-30 domain of Sdc1 is required for histone methylation and gene expression. *J Biol Chem* **285:** 595–607.

Southall SM, Wong PS, Odho Z, Roe SM, Wilson JR. 2009. Structural basis for the requirement of additional factors for MLL1 SET domain activity and recognition of epigenetic marks. *Mol Cell* **33:** 181–191.

Steward MM, Lee JS, O'Donovan A, Wyatt M, Bernstein BE, Shilatifard A. 2006. Molecular regulation of H3K4 trimethylation by ASH2L, a shared subunit of MLL complexes. *Nat Struct Mol Biol* **13:** 852–854.

Wu M, Wang PF, Lee JS, Martin-Brown S, Florens L, Washburn M, Shilatifard A. 2008. Molecular regulation of H3K4 trimethylation by Wdr82, a component of human Set1/COMPASS. *Mol Cell Biol* **28:** 7337–7344.

Wu L, Lee SY, Zhou B, Nguyen UT, Muir TW, Tan S, Dou Y. 2013. ASH2L regulates ubiquitylation signaling to MLL: *trans*-regulation of H3 K4 methylation in higher eukaryotes. *Mol Cell* **49:** 1108–1120.

Yu BD, Hess JL, Horning SE, Brown GA, Korsmeyer SJ. 1995. Altered Hox expression and segmental identity in Mll-mutant mice. *Nature* **378:** 505–508.

Zhang P, Lee H, Brunzelle JS, Couture JF. 2012. The plasticity of WDR5 peptide-binding cleft enables the binding of the SET1 family of histone methyltransferases. *Nucleic Acids Res* **40:** 4237–4246.